JOURNAL OF OPTOELECTRONICS AND ADVANCED MATERIALS Vol. 17, No. 5-6, May – June 2015, p. 634 - 639

# Growth and structural properties of Molybdenum thin films deposited by DC sputtering

JAYMIN. RAY*, T. K. CHAUDHURI
*Dr. K. C. Patel Research and Development Centre, Charotar University of Science and Technology, Changa, Anand District, Gujarat 388 421, India*

Deposition of molybdenum (Mo) thin films on soda-lime glass substrate by simple DC sputtering is reported as a function of argon pressure. The films are characterized by X-ray diffraction (XRD), Atomic force microscope (AFM), Scanning electron microscope (SEM), Resistivity and specular reflectivity measurements. XRD scan showed only strong line of Mo (110) and weak line of (211) suggesting that the films are preferred oriented along (110). AFM revealed that the films composed of spherical grains with RMS roughness of 3 to 8 nm. It is found that as the Ar pressure decreases from 3.0 to 1.3 Pa, the roughness (RMS) of films decreases from 8.2 to 3.4 nm and sheet resistance decreases from 5.3 to 1.1 Ω/sq. Roughness of films also affect the optical reflectivity. The average reflectivity of Mo films is about 55 % in the visible region. The columnar growth, observed form the cross section SEM images, indicates the dense morphology of the Mo films.

(Received July 2, 2014; accepted May 7, 2015)

*Keywords:* Molybdenum Thin film, DC Sputtering, XRD, AFM, SEM

## 1. Introduction

Molybdenum (Mo) is a silvery-grey refractory metal, which is known for it's extraordinarily resistant to heat and wear. Because of these it is used in many applications like as a electrodes, catalysts, wire filaments, casting molds, and chemical reaction vessels in corrosive environments [1]. Apart from that Mo is widely used as a thin film in various opto-electronics devices because of its low resistance and chemical inertness. In GaAs-based Metal Gate Field Effect Transistors (MESFET), silicon-based Metal Oxide Semiconductors (MOS) and Thin Film Transistor-Liquid Crystal Displays (TFT-LCDs), Mo films are used as a gate, source and drain signal lines [2,3,4]. Besides to these, Mo thin films also commonly and extensively used in thin films based solar cells as a back-contact, viz. Copper Indium Gallium Diselenide (CIGS) [5], Cadmium Telluride (CdTe) [6], and Copper Zinc Tin Sulphide (CZTS) [7]. The chemical inertness of Mo helps as a diffusion barrier between the substrate and the p-type layer even at temperature of about 600 °C [8]. As a back-contact in thin film solar cells, lower sheet resistance and the adhesion with the substrate are essential to get the efficient performance. Typical value of sheet resistance for adherent dense crystalline Mo film is 0.1 to 0.15 Ω/sq [9]. This is strongly influence by the deposition method and the deposition parameters. Magnetron sputtering is mostly used to deposit Mo thin films [10,11,12,13,14]. There are few studies available on e-beam evaporation of Mo films. [15,16]. Recently Martinez et. al. [17] observed well adherent Mo films on the glass substrate having a sheet resistance of 0.8-1 Ω/sq. That is slightly higher then the typical values but still applicable for as a back-contact in the solar cell. The XRD of those films reveals the presence of an extra phase $MoO_2$, responsible for higher values of sheet resistance as well as the non-uniform sharp-edged big grains having a surface roughness of 15-25 nm. Addition to that deviation in the sheet resistance values throughout the sample area is about 10 % due to the large source substrate distance (36 cm) and so, the lower deposition rate (4-13 Å/s).

In the sputtering technique typical distance between the source substrate is kept 5-8 cm. That provides the high deposition rate, and results in produce considerable compact, adhesive films, of course been affected by sputter process parameters like deposition pressure, sputter power and substrate temperature. Among these parameters deposition pressure affects most strongly the structure density, morphology and on the resistance of the films. Varying the deposition pressure leads to change the rate of arriving atoms and their energy and thus the quality of the films. Many studies focused on the reducing the electrical resistance and on the improvement in the adhesion with the substrate by varying the deposition pressure. Thotnton et. al. [18] successfully deposited different refractory metals like Titanium (Ti), Nickel (Ni), Tantalum (Ta) and Mo by cylindrical magnetron sputtering. They varies the deposition pressure from 0.4 to 0.15 Pa and its influence was observed in terms of the electrical resistivity, adhesion, and optical reflectance. As the deposition pressure decreased during the deposition reveals the reduction in the resistance for all metal films and improvement in the adhesion.

Considering the case for magnetron sputtered Mo films, correlation observed between the deposition pressure and the stress of the films [12,13,14]. Films deposited at lower working pressure are generally under compressive stress and hence, the films tend to buckle up or experienced a zigzag pattern like morphology. Whereas at higher pressure, films are found under the tensile stress, that is responsible for the scratches like stress lines. These higher pressure films exhibits the higher sheet resistance

with more adhesion compare to the films grown at lower working pressure. Stress free conducting films are then mandatory as a back-contact in the field of thin films based solar cell. Bilayer structure of Mo films has been tried [19,20], in which a bottom layer grown at higher pressure and the top layer grown at lower pressure. This kind of bilayer structure nearly solved the adhesion problem and showed a considerable improvement in the fabrication part of the solar cell. But the observed sheet resistance values has been slightly higher, i.e. 0.2-4 Ω/sq, compare to the 0.1-0.2 Ω/ sq for mono layer of Mo [19]. Many research groups also observed the porous bottom layer helps to diffuse sodium (Na) in the CIGS absorber layer, which again beneficial in the solar cell performance.

Recent studies are more directional toward quantify the microstructure defects for further improvement in adhesion and sheet resistance of the films. In this regards Rafaja et al. studied the influence of the impurities present in the Mo films (0.5 μm thickness) deposited by both unbalance pulsed DC and unbalance RF magnetron sputtering [21]. Chemical analysis of both RF and DC sputtered Mo films reveals the presence of the impurities like carbon, sodium, chromium, nitrogen, oxygen. This result shows increment of film resistivity, also, the observation, from Williamson hall theory, dislocation density increase linearly with the resistivity. Overall the resistivity variation influenced by the microstructure defects due to the impurities present in the films. By increasing the thickness and modifying the growth kinetics of the film one can reduce the impurities induced defects in the films. Hofer et. al. [22], prepared Mo films by DC magnetron sputtering by varying the thickness from 0.3 to 5 μm. In the case of lower thickness of Mo films the compact small grains observed at the glass-film interface. This indicates the starting point of the nucleation of atoms. As the thickness increased small grained structure act as a base to grow big compacted V-shaped columnar grains. Thicker films attributed to lower overall defect density clearly examined by the grain size of the films. In conclusion thinner films shows higher values of gross stress mainly due to the higher volume fraction of grain boundaries.

As the conductivity and the adhesion property of the dense Mo thin films played a crucial role in the performance of the solar cell. Objective of the present study is mono layer deposition of Mo by using simple DC sputtering to grow the compact, adhesive and conducting Mo films by varying the Ar deposition pressure. The structure, morphology, electrical and optical reflectivity of the Mo films are taken in to the account for optimizing the growth condition of the Mo films.

## 2. Experimental detail

Mo thin films are prepared on soda lime glass substrate (25 mm × 25 mm) by using circular DC sputtering system, (15F6 HINDHIVAC, India), at different argon (Ar) pressure.

Soda-lime glass substrates are cleaned by ultrasonic bath of neutral pH detergent, deionized water and methanol, and dried with flow of dry-air successively. The cleaned glass substrates are stored in air tight container before the deposition. The distance between Mo target (2 inch diameter, 5 mm thick) and the substrate is kept 50 mm. DC power set to 90 W and deposition time is 120 min. for all depositions. The pressure of the chamber is varied from 1.3 to 3.0 Pa using Argon (Ar) gas flow which is controlled by the needle valve. Before initiating the actual deposition of Mo thin films, the target was pre-sputtered for 5 minutes to remove the surface contamination.

Structure of deposited Mo thin films are characterized using X-ray Diffractometer (XRD) (D2Phaser, Bruker) in 2θ range of 30° - 80°, at a scan-rate of 0.02° $s^{-1}$, using Ni-filtered CuKα radiation. The surface morphology of the films is examined by Atomic Force Microscope (AFM) (Easyscan2, Nanosurf) in tapping mode and Scanning Electron Microscopy (SEM) (Leo s-440i). The electrical resistivity was measured using the Van der Pauw method and specular reflectivity was measured using UV-VIS-NIR spectroscopy (UV-3600, Shimadzu) in the wavelength range of 400-1200 nm.

## 3. Results and discussion

Simple visual inspection of the deposited Mo films is employed, indicates the mirror like appearance with at shiny bright surface. Then the adhesion of the film to the substrate is checked by simple adhesive tape test. Adhesive tape strips of same lengths are glued uniformly on the film and stripped with approximately equal amount of force. All films showed good adhesion with the substrate except the films grown at higher pressure i.e. peeled off partially from substrate.

The structural quality of deposited Mo films is found from XRD patterns (as shown in Fig. 1), by analyzing the intensity and the Full width half maxima (FWHM) of the main diffraction peak. XRD patterns contain only two peaks at 40.02° and 72.72°. The d-values for the peaks well match with the standard JCPDS card 01-1208 indicating cubic structure of Mo. On the basic of that peaks at 40.02° and 72.72° are assigned to reflection due to (110) and (211) planes. A linear increment in the intensity ratio of (110) and (211) peak indicate a preferred (110) orientation which has also been observed by klabunde et al. [23]. With that the decrement in the FWHM of the major diffraction peak indicates improvement in the crystallinity of the grains, as the working pressure of Ar decreases.

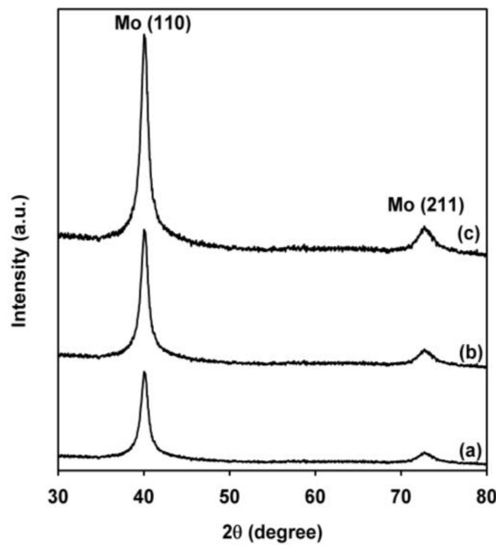


*Fig. 1. XRD plot of Mo thin films grown at different Ar working pressure: (a) 3.0 Pa, (b) 2.0 Pa, and (c) 1.3 Pa*

Using the values of FWHM, the crystallite size (D), is calculated using the Scherrer's formula [24],

$$D = \frac{K\lambda}{\beta_{2\theta}\cos\theta} \qquad (1)$$

Where,
K = constant taken to be a 1,
$\lambda$ = X-ray wavelength = 1.5418 Å,
$\beta_{2\theta}$ = FWHM of the (110) peak,
$\theta$ = Bragg angle of reflection,

The average crystallite sizes of Mo thin films deposited at different Ar pressure is shown in Table 1. It is found that the crystallite size increases as the Ar pressure decreases. Improvement in the crystallite size depends mainly on the deposition or condensation rate and the deposition temperature. The deposition time constant for all sets of films, so the deposition temperature affect equally on the growth of film. By varying the Ar working pressure, the deposition rate varies. At lower pressure, at 1.3 Pa, the collisions of the sputtered particle with the gas will be reduced and therefore the rate of deposition increases. Owing to this, the sputtered particles with its improved energy reduce its arrival angle to the substrate. Thus, the possibility of the formation of inter-granule void reduces, which, in turn, results in the dense structure of the grains and hence the improvement in the crystallinity of the film [25].

*Table 1. Average crystallite sizes and the strain variation in Mo thin film influence by Ar working pressure.*

| Ar working pressure (Pa) | FWHM (degree) | Average crystallite size (nm) | | Strain from W-H plot ($\varepsilon \times 10^{-3}$) |
|---|---|---|---|---|
| | | Scherrer's formula | Williamson-Hall | |
| 1.3 | 0.943 | 9.2 ± 0.2 | 8.6 ± 0.2 | 10 |
| 2.0 | 0.991 | 8.0 ± 0.1 | 7.5 ± 0.1 | 15 |
| 3.0 | 1.063 | 7.4 ± 0.2 | 6.8 ± 0.2 | 18 |

\

The lattice constant of Mo films is found to be a = 5.941 Å, which almost matches with the standard data $a_0$ = 5.936 Å. Deviation in the lattice parameter "a" from the standard data indicates the crystallites may be under some strain. However, small may be with crystallite size, the presence of non uniform strain in the Mo film contribute to broadening of the XRD peak. This means crystallite size derived from Scherrer's formula always slightly more than its actual sizes. If in this case, than from Williamson-Hall (W-H) plot (shown in Fig. 2) one can find the strain present in the crystallites using equation 2 [26],

$$\beta_{2\theta}\cos\theta = \frac{K\lambda}{D_{WH}} + C\varepsilon\sin\theta \qquad (2)$$

Where,
$\beta_{2\theta}$ = FWHM of the (110) peak,
$\theta$ = Bragg angle of reflection,
$\lambda$ = 1.5418 Å, X-ray wavelength,
$D_{WH}$ = Average crystallite size
$\varepsilon$ = Strain

Linear slope of equation 2 gives the value of strain and from the intercept $D_{WH}$ is been calculated. Average crystallite size calculated from the W-H plot is slightly lower than the Scherrer's equation. It has been confirmed the broadening of X-ray peak is due to the both the strain and the crystallite size. The strain value observed from W-H plot, shown in Table 1. At higher working pressure the value of the strain is 18.1 × $10^{-3}$, which is slightly higher that the films deposited at lower pressure.

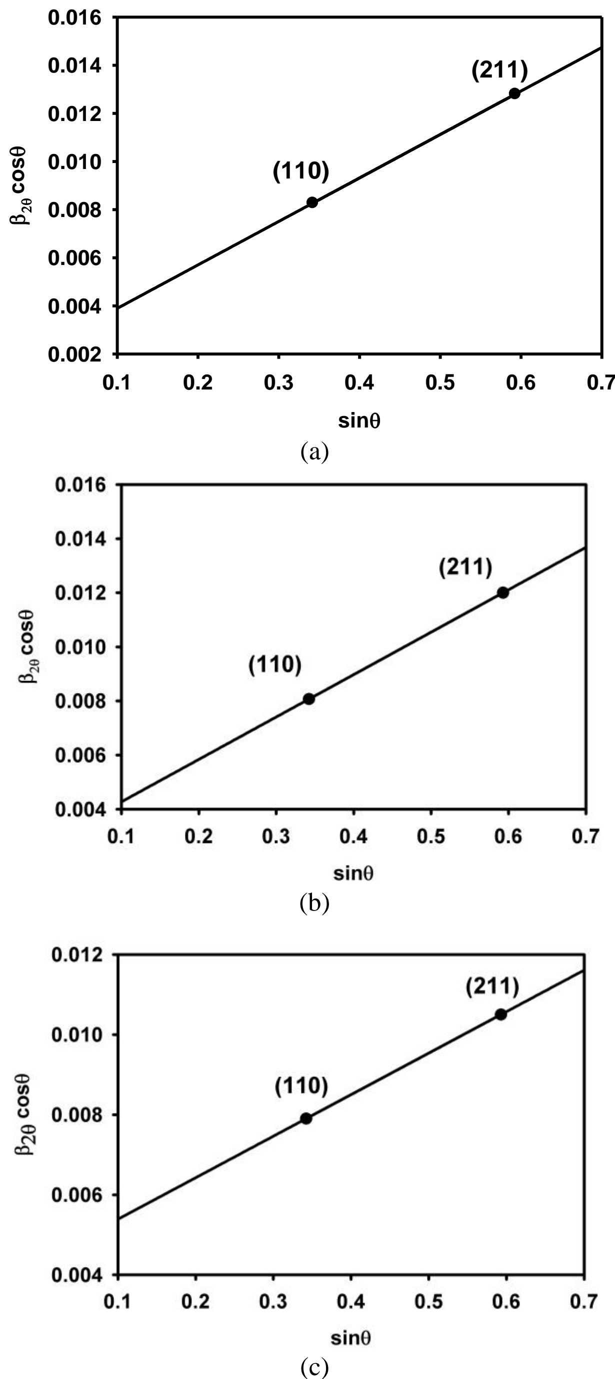


*Fig. 2. W-H plot of Mo thin films deposited at different Ar working pressure: (a) 1.3 Pa, (b) 2.0 Pa, and (c) 3.0 Pa*

The microstructure morphology of the Mo films observed using AFM and SEM (top-view), as shown in Fig. 3.

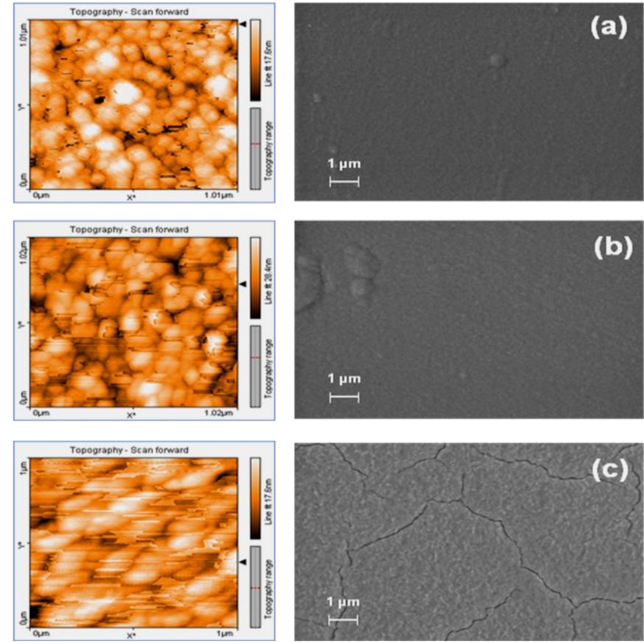


*Fig. 3. AFM and SEM (top-view) images of Mo thin films grown at different Ar working pressure: (a) 1.3 Pa, (b) 2.0 Pa, and (c) 3.0 Pa*

The films grows at lower working pressure has dense, uniform granule surface morphology. As the pressure increases the non uniformity (from AFM) and cracks (from SEM) in the films is observed that confirms the presence of the strain in the films. The surface roughness, over 1 $\mu m^2$, for less strained morphology, i.e. films grown at lower working pressure, the surface roughness is around 3 nm and as the pressure increases the surface roughness increases to around 8 nm, due to the strained non uniformed surface structure [27], This is because of the multiple collision between the sputtered particles and the Ar ions at higher pressure increases, which leads to reduction in the kinetic energy of the sputtered particles. And so, the average arrival angle of the particles at the substrate.

The optical reflectivity of the back-contact is also an essential parameter for solar cell efficiency. Reflectance of the back-contact helps light photons absorbs back into the absorber. The optical reflectance affected by the change in the surface roughness of the film. It is clear that higher Ar flow rate can modify the surface of the film, decline the optical quality of the film, which supports the morphological and electrical studies of the presented work. At higher working pressure the value of surface roughness is 8 nm having a average reflectance of about 28-60 % and at a lower working pressure 3 nm surface roughness and 40 -70 % about average reflectance.

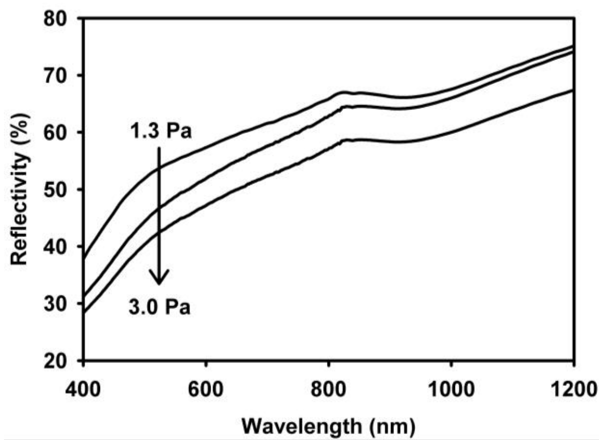


*Fig. 4. Optical reflectivity of Mo thin films as a function of Ar working pressure.*

Cross-sectional SEM images of Mo thin films as shown in Fig. 5 reveals columnar structure with elongated and faceted surface characteristic.

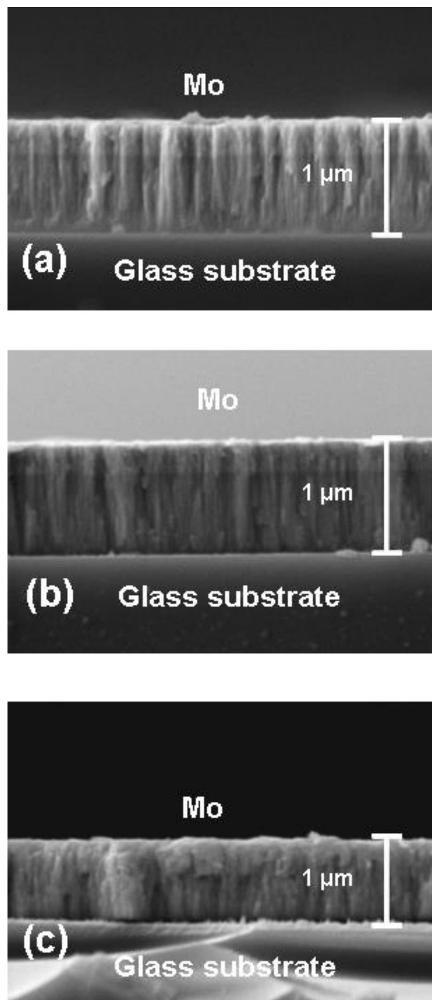


*Fig. 5. SEM images of Mo thin films grown at different Ar working pressure: (a) 1.3 Pa, (b) 2.0 Pa, and (c) 3.0 Pa*

The similar thickness for all deposited films is confirmed, i.e. about 1 μm from cross section SEM. Clear tightly packed uniformly distributed columns with nearly equal height to the thickness of the films are observed at lower working pressure indicates. Similar kind of columnar growth have been reported for Mo films deposited by sputtering and e-beam, with the grain sizes ranging from 3 to 5 nm (sputtering [28,29]) to 40 nm (e-beam [30]). At higher pressure boundaries of the grains seems to be diffuse or difficult to distinguish, in fact an agglomeration of grains occurs.

Furthermore, the densely packed surface morphology results decrease in the sheet resistance of the film. The variation in sheet resistance of the Mo films as a function of the deposition pressure is shown in Fig. 6. The lowest resistivity value found for the Mo films grown at lower presser is 1.1 Ω/sq.

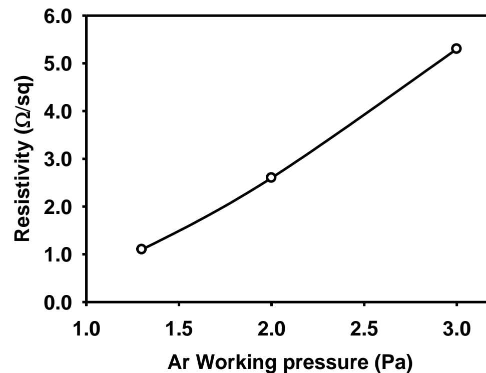


*Fig. 6. Variation in sheet resistance of Mo films as a function of Ar working pressure*

It is observed that the decrease in resistivity of the Mo films is accompanied by an increase of the grain size, clearly observed from cross section SEM. Grain size improvement results in reduction of the grain boundary potential barrier's height, as well as the number of grain boundaries, which enhance the carrier mobility. At lower working pressure the columnar growth improves the electrical conductance because of reduced grain boundaries. Agglomeration of the grains, at higher working pressure, increases the grain boundaries, which act as a barrier for the electrical transport, which, in turn, leads to increase of the resistivity. Thornton et al. [18] also observed that decrease in optical reflectivity and increase in resistivity of Mo thin film deposited at different working pressure was mainly from the stress.

## 4. Conclusion

Mo thin films are deposited on soda lime glass substrate using simple DC sputtering. The influence of Ar controlled working pressure was observed by the structural, morphological, electrical, and optical studies. The observations indicate that the metallic Mo thin films showed a better crystallinity, morphology, conductivity, and reflectivity at a lower working pressure (1.3 Pa). The

typical Values of resistivity is 1.1 Ω/sq, the surface roughness of 3.4 nm and near to 55% reflectivity in the visible region for Mo thin films. These results of Mo thin films are been beneficial as a back-contact layer for solar cells.

**Acknowledgement**

The authors are thankful to President and Provost of Charotar University of Science and Technology (CHARUSAT) for supporting this work.

## References

[1] J. Emsley, Nature's Building Blocks, Oxford University Press, Oxford (2001).
[2] U. Schmid, H. Seidel, Thin Solid Films **489,** 310 (2005)
[3] Y.G Shen, Materials Science and Engineering: A, **359,** 158 (2003)
[4] Yee-Wen Yen, Yu-Lin Kuo, Jian-Yu Chen, Chiapyng Lee, Chung-Yu Lee, Thin Solid Films, **515,** 7209 (2007)
[5] P. Jackson, D. Hariskos, E. Lotter, S. Paetel, R. Wuerz, R. Menner, W. Wischmann, M. Powalla, Progress in Photovoltaics: Research and Applications, **19,** 894 (2011)
[6] I. Mautlionis, S. Han, J.A Drayton, K.J Price, A.D Compaan, Proceedings of the Materials Research Symposium on II-VI compound semiconductor photo voltaic materials, **668,** H8.23.1 (2001)
[7] T.K. Todorov, J. Tang, S. Bag, O. Gunawan, T. Gokmen, Y. Zhu, D.B. Mitzi, Adv. Energy Mater. **3,** 34(2013)
[8] S. Raud, M. -A. Nicolet, Thin Solid Films **201,** 361 (1991)
[9] Ju-Heon Yoon, Kwan-Hee Yoon, Won Mok Kim, Jong-Keuk Park, Young-Joon Baik, Tae-Yeon Seong Jeung-hyun Jeong J. Phys. D: Appl. Phys. **44,** 425302 (2011)
[10] F. A. Abou-Elfotouh, L. L. Kazmerski, R. J. Matson, D. J. Dunlavy, T. J. Coutts., J. Vac. Sci. Tech. A **8,** 3251 (1990)
[11] D.W. Niles, A.J. Nelson, C.R. Schwerdtfeger, H. Höchst, D. Rioux, Mat. Res. Soc. Symp. Proc. **260,** 299 (1992)
[12] E. Moons, T. Engelhard, D. Cahen, J. Electr. Mat. **22,** 275 (1993)
[13] A.A. Kadam, N.G. Dhere, P. Holloway, E. Law, J. Vac. Sci. Technol. A **23,** 1197 (2005)
[14] D.W. Haffman, J.A. Thornton, J. Vac. Sci. Technol. **20,** 355 (1982)
[15] H. Oikawa, Y. Nakajima, J. Vac. Sci. Technol. **14,** 1153 (1977)
[16] N. Tralshawala, R.P. Brekosky, M.J. Li, E. Figueroa-Feliciano, F.M. Finkbeiner, M. A. Lindeman, C.M. Stahle, C.K. Stahle, IEEE Trans. Appl. Supercond. **11,** 755(2001)
[17] M.A. Martinez, C. Guillén, Journal of Materials Processing Technology, **143,** 326 (2003)
[18] J.A. Thornton, D.W. Hoffman, J. Vac. Sci. Technol. **14,** 164 (1977)
[19] J.H. Scofield, A. Duda, D. Albin, B.L. Ballard, P.K. Predecki, Thin Solid Films, **260,** 26 (1995)
[20] Ju-Heon Yoon, Tae-Yeon Seong, Jeung-hyun Jeong, Prog. Photovolt: Res. Appl. **21,** 58 (2013)
[21] D. Rafaja, H. Köstenbauer, U. Mühle, C. Löffler, G. Schreiber, M. Kathrein, J. Winkler, Thin Solid Films **528,** 42 (2013)
[23] A.M. Hofer, J. Schlacher, J. Keckes, J. Winkler, C. Mitterer, Thin Solid Films **99,** 149 (2014)
[24] F. Klabunde, M. Löhmann, J. Bläsing, T. Drüsedau, J. Appl. Phys **80,** 6266 (1996)
[25] B.D. Cullity, S.R. Stock, Elements of X-Ray Diffraction, Prentice-Hall Inc. (2001).
[26] G. Hass, R.E. Thun, Physics of thin films, Academic press, New York and London (1966).
[27] G.K. Williamson, W.H. Hall, Acta. Metall. **1,** 22 (1953)
[28] Lourdes Fàbrega, Iván Fernández-Martínez, María Parra-Borderías, Óscar Gil, Agustín Camón, Raquel González-Arrabal, Javier Sesé, José Santiso, José-Luis Costa-Krämer, and Fernando Briones, IEEE Transactions on Applied Superconductivity, **19(6),** 3779 (2009)
[29] T.J. Vink, M.A.J. Somers, J.L.C. Daams, A.G. Dirks, J. Appl. Phys., **70(8),** 4301 (1991)
[30] N.Y. Fogel, O.A. Koretskaya, A.S. Pokhila, V.G. Cherkasova, E.I. Buchstab, S.A. Yulin, J. Low Temp. Phys., **22(4),** 277 (1996)
[31] H. Oikawa, T. Tsuchiya, J. Vac. Sci. Technol. **15**(3) 1117 (1978)

*Corresponding author : jayminray.rnd@charusat.ac.in